

Design, synthesis and trypanocidal activity of lead compounds based on inhibitors of parasite glycolysis

Matthew W. Nowicki,^{a,b} Lindsay B. Tulloch,^b Liam Worrall,^b Iain W. McNae,^b Véronique Hannaert,^c Paul A. M. Michels,^c Linda A. Fothergill-Gilmore,^b Malcolm D. Walkinshaw^b and Nicholas J. Turner^{a,*}

^aSchool of Chemistry, University of Edinburgh, King's Buildings, West Mains Road, Edinburgh, EH9 3JJ, UK

^bStructural Biochemistry Group, Institute of Structural and Molecular Biology, University of Edinburgh, King's Buildings, Mayfield Road, Edinburgh EH9 3JR, UK

^cResearch Unit for Tropical Diseases, de Duve Institute and Laboratory of Biochemistry, Université Catholique de Louvain (UCL), Avenue Hippocrate 74, B-1200 Brussels, Belgium

Received 13 January 2008; revised 2 March 2008; accepted 11 March 2008
Available online 21 March 2008

Abstract—The glycolytic pathway has been considered a potential drug target against the parasitic protozoan species of *Trypanosoma* and *Leishmania*. We report the design and the synthesis of inhibitors targeted against *Trypanosoma brucei* phosphofructokinase (PFK) and *Leishmania mexicana* pyruvate kinase (PyK). Stepwise library synthesis and inhibitor design from a rational starting point identified furanose sugar amino amides as a novel class of inhibitors for both enzymes with IC₅₀ values of 23 μM and 26 μM against PFK and PyK, respectively. Trypanocidal activity also showed potency in the low micromolar range and confirms these inhibitors as promising candidates for the development towards the design of anti-trypanosomal drugs.

© 2008 Elsevier Ltd. All rights reserved.

1. Introduction

The parasitic protozoa *Trypanosoma* and *Leishmania* are the causative agents of the highly disabling and often fatal diseases, such as African sleeping sickness, Chagas' disease and leishmaniasis. Millions of people are at risk in the areas of Africa, South America and Asia where these diseases are endemic. Unfortunately, current drugs are far from satisfactory as they often possess toxic side effects, are ineffective against certain disease forms and may require expensive administration procedures; in addition, resistance to these drugs is becoming an increasingly common problem.¹

In the last two decades, experimental approaches such as gene cloning, protein crystallography and RNA interference have been introduced to define and validate po-

tential new drug targets in Trypanosomatidae. Glycolysis appears to provide an excellent therapeutic target because it is essential to bloodstream form Trypanosomatidae as the only catabolic source of ATP.^{1,2} Furthermore, due to the evolutionary distance between Trypanosomatidae and humans,³ the parasite enzymes within the pathway possess distinct properties that differentiate them from their mammalian counterparts, and which could be exploited in the design of parasite-specific drugs.⁴ The unique organisation of the glycolytic pathway in trypanosomatids, with most of the enzymes present in peroxisome-like organelles called glycosomes, is correlated with exploitable differences. Thus, the compartmentalisation has resulted in different kinetic properties and activity regulation mechanisms that correspond to differences in enzyme structure.⁴ Phosphofructokinase (PFK) and pyruvate kinase (PyK) are validated as two such enzymes which could, therefore, be targeted.^{2,4–6}

PFK catalyses the phosphorylation of fructose 6-phosphate (F6P) to produce fructose 1,6-bisphosphate (F1,6BP). The parasite enzyme exists as a homotetramer and, under physiological conditions, the reaction is

Keywords: Pyruvate kinase; Phosphofructokinase; Inhibitors; *Leishmania*; *Trypanosome*; Parasite; Drug development; Glycolysis.

* Corresponding author at present address: School of Chemistry, Manchester Interdisciplinary Biocentre, 131 Princess Street, Manchester M1 7DN, UK; e-mail: Nicholas.Turner@Manchester.ac.uk

essentially irreversible. Recently, the crystal structure of *Trypanosoma brucei* PFK (*Tb* PFK) has been solved⁷ showing striking differences from human PFK. Not only is there a low sequence identity between the two enzymes (<25% identical), but the *Tb* PFK structure shows an additional domain and loops, including a loop adjacent to the active site which is not present in the human structure. Such differences are important in being able to design selective inhibitors of the parasitic PFK targeted towards the active site. Indeed, preliminary attempts to design inhibitors of trypanosomatid PFK have had promising results. Analogues of 2,5-anhydro-D-mannitol bearing various arylamino groups at position 1 (structurally similar to F1,6BP, [Scheme 1](#)) have shown weak inhibitory activity by reversibly binding at the ATP and F6P binding sites,⁸ the most active of which bears a phosphate at the 6-position. Although in most eukaryotes, including humans, fructose 2,6-bisphosphate (F2,6BP) is a potent activator of PFK, this is not the case in trypanosomatids. Thus, fructose-phosphate analogues are expected to affect trypanosomatid PFKs through the active site, not the effector site.

PyK catalyses the conversion of phosphoenolpyruvate (PEP) to pyruvate whilst producing ATP. Trypanosomatid PyK is allosterically regulated by F2,6BP which induces conversion to the active R-state of the enzyme from the inactive T-state.⁶ In contrast, mammals possess four isoenzymes of PyK, one of which (M1) is constitutively active and the other three (M2, L and R) are regulated by F1,6BP.⁴ Although *Tb* PyK can be activated by F1,6BP, the concentrations needed are 2000-fold higher than those needed for F2,6BP. The determination of the crystal structure of *Leishmania mexicana* PyK (*Lm* PyK)⁹ and comparisons with human PyKs have highlighted significant differences at the effector site that would, therefore, appear to be another promising target.

The starting point for inhibitor development was the synthesis of a wide range of compounds based on the *N*-substituted-1-amino-2,5-anhydro-1-deoxy-D-mannitol

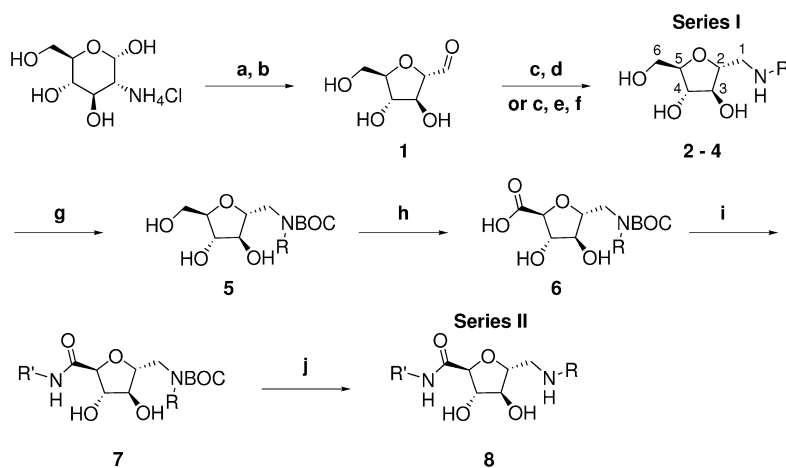
scaffold (series I, [Scheme 1](#)) primarily by substitution at the 1-position. These compounds were screened against both *Tb* PFK and *Lm* PyK (due to the structural similarity between F6P, F2,6BP and the inhibitor scaffold). A further round of inhibitor development involved functionalising the 6-position through selective oxidation, followed by amide coupling.

The results that are reported herein are an important step towards the overall goal of producing trypanocidal drugs. Due to the high species similarities of PFKs and of PyKs within the Trypanosomatidae (>70% sequence identity for each enzyme), it is likely that inhibitors that are active against one parasite, would also be efficacious against *Trypanosoma cruzi* and the various pathogenic *Leishmania* species.

2. Chemistry

Derivatives in series I ([Scheme 1](#)) were prepared in two steps following the procedures described by Claustre et al.^{8,10} The nitrous acid deamination of D-(+)-glucosamine hydrochloride, an adaptation of the Horton and Philips method,¹¹ proceeded in good yield and was followed by reductive amination reactions using various primary amines, adapted for multi-parallel synthesis (low to moderate yields, purified using mass-directed purification). Amines in series I were screened against *Tb* PFK and *Lm* PyK.

Modification of the reductive amination step was necessary in order to improve yields for subsequent inhibitor development and the generation of series II; this improvement was achieved using a solid supported borohydride resin and the amine scavenger resin, 4-benzoybenzaldehyde polystyrene.^{12–14} The mannonamide derivatives in series II were prepared in four steps from amines **2m** and **3m**. Boc protection of the secondary amine occurred in moderate yields, followed by the key TEMPO mediated selective oxi-



Scheme 1. Reagents and conditions: (a) NaNO₂, Amberlite 120 H⁺, 0 °C, 18 h; (b) Dowex CO₃²⁻; (c) RNH₂, (20 min for parallel synthesis, 2 h when using solid phase reagents); (d) NaBH₃CN, HCl, 1.5 h; (e) borohydride resin, 24 h; (f) 4-benzoybenzaldehyde polystyrene, 72 h; (g) Boc₂O, DMAP, dioxane, MeCN, H₂O, 0 °C, 2 h; (h) TEMPO, KBr, TBACl, NaOCl, NaCO₃, brine, DCM, 0–25 °C, 2–24 h; (i) R'NH₂, EDCI, HOBT, DIPEA, DCM, 20 h; (j) TFA, DCM, 2 h.

dation of the 6-hydroxyl to the corresponding acid. The biphasic oxidation was an adaptation of the method set out by Davis and Flitsch¹⁵ and gave low to moderate yields, although this could have been due to the difficulty in extracting the target acids from the aqueous phase. Subsequent amide coupling using EDCI, HOBt and DIPEA^{16,17} and Boc deprotection gave the series II sugar amino amides which were screened against either *Tb* PFK, *Lm* PyK or both, depending upon the R group specificity from the series I screen.

3. Results and discussion

3.1. Library 1

The discovery that analogues derived from 2,5-anhydro-D-mannitol showed weak inhibition against *Tb* PFK⁸ led to further investigation into inhibitors of this type (series I). Series I was additionally screened against *Lm* PyK because F1,6BP is not only the product of PFK, but is also an effector of PyK.

Inhibitory activities of 55 amine derivatives of 2,5-anhydro-D-mannitol in series I against *Tb* PFK are reported in Table 1. All compounds (tested at 5 mM) showed inhibition to some extent, with 13 compounds causing greater than 50% inhibition. Compound **2m** (2,5-anhydro-1-deoxy-(3,4-dichlorobenzylamino)-D-mannitol) was particularly effective by reducing activity to 5%. Compound **2m** therefore possessed at least a 6-fold better potency than other amines in this screen. The IC₅₀ for **2m** was determined to be 0.41 ± 0.05 mM, a value comparable to the most potent analogue described by Claustre et al.⁸ (R = 3-nitrophenyl, IC₅₀ = 0.45 mM). However, it should be noted that the 3-nitrophenyl derivative is phosphorylated at the 6-position, and when non-phosphorylated had an almost doubled IC₅₀ value of 1.1 mM. The results from series I thus identified an analogue with a greatly optimised R-group (3,4-dichlorobenzyl) which was incorporated in further inhibitor development leading to the synthesis of series II.

Screening of series I against *Lm* PyK gave 16 compounds with greater than 50% inhibition (Table 1), with eight compounds reducing their activity to 30% or less. Interestingly, it appears that the most active of these bear hydrophobic groups at the 1-position. It is also noticeable that whilst the majority of series I compounds inhibit PyK, there are a small number of compounds that activate PyK (remaining activity greater than 100%), which would suggest that the series may bind to the effector site rather than binding to the active site of the protein. (Compounds that bind to the active site would only exhibit inhibition of the enzyme, whilst those that bind to the effector site could exhibit either inhibition or activation.)

IC₅₀ values of ten of the more active compounds were determined and are shown in Table 1. The majority of the hits showed only weak inhibitory activity (in the

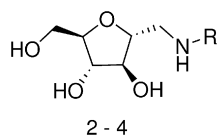
low millimolar range), however, amine **3m** gave an IC₅₀ of 71 μ M which is over 10-fold more potent than any other inhibitors from the same series. This difference is striking and points to the suggestion that there is a hydrophobic pocket located in the effector site which allows for a highly specific interaction with the cycloheptyl moiety of **3m**. Of the other amines in series I that bear a carbocycle at the 1-position, all showed much lower potency than **3m** indicating that the hydrophobic interaction is likely to be specific. Moreover, amine **3m** is a novel inhibitor of *Lm* PyK and was an ideal candidate to take forward for the development of series II.

3.2. Library 2

Table 2 shows inhibitory activity of compounds in series II against both *Tb* PFK and *Lm* PyK. All members of series II are sugar amino amides, derived from the two best hits (**2m** and **3m**) from the series I screen.

Activity results against *Tb* PFK showed a noticeable improvement over series I. The initial screen was performed at an inhibitor concentration of 1 mM (in contrast to the 5 mM concentration used for series I) and all amides tested exhibited an improved level of inhibition over amine **2m**. Determined IC₅₀ values for four of the best inhibitors demonstrate around a 10-fold increase in potency compared to amine **2m** and to previous inhibitors of *Tb* PFK⁸ confirming that the sugar amino amides in series II are a new class of *Tb* PFK inhibitor. Amide **8e** exhibited the greatest inhibition with an IC₅₀ of 23 μ M although other amides displayed comparable potency (low micromolar) showing that the introduction of the amide group has a marked effect upon potency of the series II analogues.

Figure 1a depicts a representation of potential interactions of inhibitor **8e** with the F6P binding site of *Tb* PFK (pdb id: 2HIG). The model has been generated by positioning the furanose ring of **8e** in the position in which F1,6BP is found in the *E. coli* PFK structure (1PFK)¹⁸ so that the 3,4-*trans*-dihydroxyl moiety is clamped by residue Glu325. In the orientation shown, the amide is making three hydrogen bonding interactions with Arg173 and Arg383, which inhibitor **2m** would not be able to make. Thus, coupled with the extra hydrophobic bulk of the series II inhibitors, the interactions they gain could account for their increase in potency over the series I inhibitors. Interestingly, it can be seen from the results in Table 2 that when the 3,4-dichlorobenzyl group and the R' group are reversed (as in the case for amides **8f** and **8h**) little change in potency is observed (IC₅₀ = 80 μ M for **8f** and 49 μ M for **8h**). An explanation for this result could be that either the hydrogen bonding interactions gained by the presence of the amide group compensate for the switching of the optimised 3,4-dichlorobenzyl group, or that the sugar amino amide inhibitors have a different binding mode compared to that of **2m**. Due to the pseudo-C2 symmetry of the furanose scaffold of the series II inhibitors, it is likely that the 3,4-dichlorobenzyl group is actually the optimal group for the 6-position, rendering the 1-position susceptible to further optimisation. A

Table 1. Screening results of series I against *Tb* PFK and *Lm* PyK

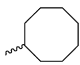
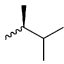
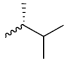
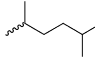
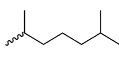
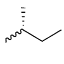
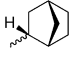
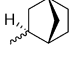
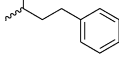
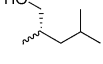
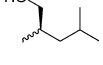
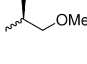
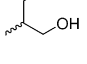
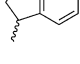
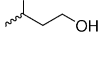
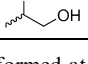
Compound	R	PFK screen (% r.a.) ^a	IC ₅₀ vs PFK (mM) ^b	PyK screen (% r.a.) ^a	IC ₅₀ s vs PyK (mM) ^b
2a		58	—	—	—
2b		85	—	88	—
2c		65	—	81	—
2d		65	—	71	—
2e		73	—	90	—
2f		61	—	89	—
2g		68	—	100	—
2h		30	—	89	—
2i		46	—	105	—
2j		63	—	42	—
2k		59	—	107	—
2l		57	—	100	—
2m		5	0.41	43	—
2n		69	—	—	—
2o		87	—	103	—
2p		59	—	85	—
2q		75	—	—	—
2r		87	—	52	4.1

(continued on next page)

Table 1 (continued)

Compound	R	PFK screen (% r.a.) ^a	IC ₅₀ vs PFK (mM) ^b	PyK screen (% r.a.) ^a	IC ₅₀ s vs PyK (mM) ^b
2s		83	—	72	—
2t		70	—	26	2.5
2u		64	—	80	—
2v		77	—	97	—
2w		33	—	49	—
2x		57	—	60	—
2y		52	—	103	—
2z		62	—	36	1.2
3a		54	—	43	4.3
3b		—	—	40	—
3c		—	—	22	3.5
3d		—	—	25	0.9
3e		—	—	36	—
3f		—	—	53	—
3g		—	—	58	—
3h		—	—	84	—
3i		69	—	83	—
3j		—	—	30	1.5
3k		33	—	34	1.5
3l		58	—	125	—
3m		63	—	19	0.071

Table 1 (continued)

Compound	R	PFK screen (% r.a.) ^a	IC ₅₀ vs PFK (mM) ^b	PyK screen (% r.a.) ^a	IC ₅₀ s vs PyK (mM) ^b
3n		64	—	57	—
3o		49	—	26	2.3
3p		51	—	86	—
3q		44	—	115	—
3r		87	—	80	—
3s		—	—	28	—
3t		—	—	47	—
3u		40	—	19	1.5
3v		73	—	95	—
3w		64	—	73	—
3x		52	—	86	—
3y		35	—	82	—
3z		36	—	90	—
4a		41	—	86	—
4b		47	—	85	—
4c		47	—	59	—

Screenings were performed at an inhibitor concentration of 5 mM; r.a. = remaining activity.

^a Screenings performed in triplicate where sufficient compound was available. In general, SD <5%.

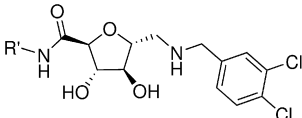
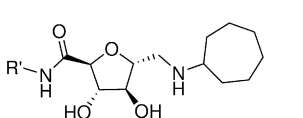
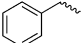
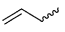
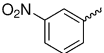
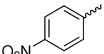
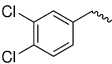
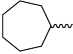
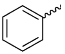
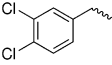
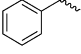
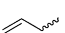
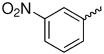
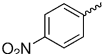
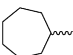
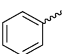
^b R² values >0.99.

proposed extension of this library could, therefore, include sugar amino amides where the 1-position is modified in the presence of the 6-position 3,4-dichlorobenzylamido group.

Results of the screen of series II against *Lm* PyK showed comparable results to the best hits from the series I screen. Unlike for *Tb* PFK, the introduction of the

amide group does not appear to have as great an effect upon inhibition although a high proportion of hits are observed, signifying the importance of the cycloheptyl group on potency. Almost a 3-fold improvement in potency is seen over the best hit from series I, with **8m** having an IC₅₀ value of 26 μM. In the case where the optimised cycloheptyl group and the R' group are reversed (as for compounds **8m** and **8f**), all potency is lost

Table 2. Screening results of series II against *Tb* PFK and *Lm* PyK

<div style="display: flex; justify-content: space-around; align-items: center;"> <div style="text-align: center;">  <p>A</p> </div> <div style="text-align: center;">  <p>B</p> </div> </div>						
Compound	General Structure	R'	PFK screen (% r.a.) ^a	IC ₅₀ vs PFK (μM) ^b	PyK screen (% r.a.) ^a	IC ₅₀ vs PyK (μM) ^b
8a	A		4.0	—	—	—
8b	A		2.0	50	—	—
8c	A		1.7	—	—	—
8d	A		0.8	—	—	—
8e	A		0.9	23	—	—
8f	A		4.7	80	88.2	—
8g	A		5.5	—	—	—
8h	B		0.4	49	—	—
8i	B		—	—	11.5	—
8j	B		—	—	19.1	—
8k	B		—	—	7.6	53
8l	B		—	—	12.5	—
8m	B		—	—	1.9	26
8n	B		—	—	24.8	—

Inhibitor concentration was 1 mM for PFK screen and 5 mM for PyK screen; r.a. = remaining activity.

^a Screenings performed in triplicate where sufficient compound was available. In general, SD <5%.

^b R² values >0.99.

(only 12% inhibition at a concentration of 5 mM) clearly indicating that the 1-position is optimised for the cycloheptyl group, and that the hydrophobic pocket identified in the series I screen cannot accommodate an amide functionality (likely to be caused by electrostatic repulsion of the amide carbonyl).

Figure 1b shows a model of **8m** in the effector site of *Lm* PyK (pdb id: 1PKL). Initially, attempts were made to

model the furanose ring of **8m** in the same orientation as F1,6BP in the yeast PyK structure (pdb id: 1A3W). However, in this position **8m** is unable to occupy the effector site due to severe steric clashes. It should be noted that the position of the flexible loop in the yeast structure (R-state) is in a more open conformation compared to that in the *Lm* structure (T-state). However, steric clashes are not just caused by the flexible loop, but are also caused by other clashes with both cyclohep-

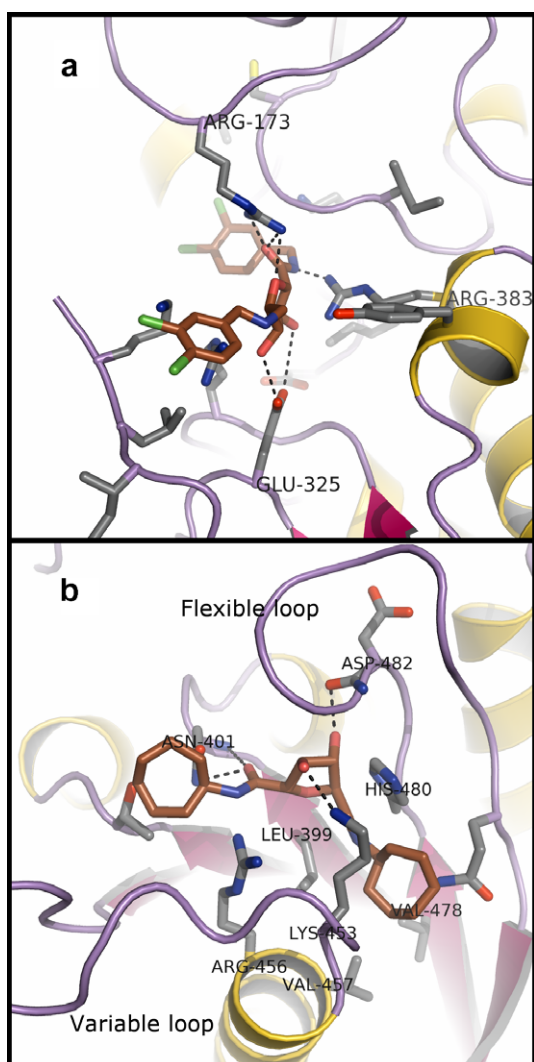


Figure 1. Models of potential interactions of (a) **8e** with the active site of *Tb* PFK, and (b) **8m** with the effector site of *Lm* PyK.

tyl moieties of **8m**. Therefore, a simple overlay of the furanose rings of F1,6BP and **8m** seems unlikely. An alternative mode of binding was discovered by rotating the sugar scaffold through 180 degrees. The cycloheptylamino moiety now occupies a hydrophobic pocket created by residues Leu399, Val457, Val478 and the C₄ chain of Lys453, with the furanose scaffold still making interactions with the flexible loop and possibly the side chain of Lys453. The mechanism for allosteric control of *Lm* PyK is not fully understood, although it is likely to arise via conformational changes in the effector site (movement of the ‘flexible’ and ‘variable’ loops, Figure 1b) which cause further conformational changes to favour binding of the substrate in the active site.^{9,19} Our docked model (Fig. 1b) suggests that the inhibitors of *Lm* PyK may bind to and stabilise the inactive form of the enzyme, and with the cycloheptyl moiety anchored in the hydrophobic pocket, residues Lys453 and His480 are unable to interact with an electronegative group (such as the 2-phosphate of F2,6BP) and, therefore, the transition from T to R state is restricted. The hydrophobic interactions themselves are also likely to

inhibit the necessary activating conformational changes. The increased potency observed between inhibitor **3m** and the series II inhibitors could be largely due to the increase in hydrophobic bulk. Therefore, **8m** is a good starting point for lead optimisation, particularly for alternative modifications at the 6-position.

3.3. In vitro parasite screens

An important part of current drug design is to verify the inhibitor’s action on the biological system for which it was designed. Even at such an early stage in the drug design process, evidence of activity against target cells is desirable to help with subsequent lead identification and modification as well as to confirm the desired biological effect. Information gained may also help with identifying inhibitors that have the correct physical properties to enter the target cells as these properties could play a crucial role in further rounds of inhibitor modification. Table 3 shows the results of some series I and II inhibitors tested against cultured *T. brucei* cells (strain 427).

Significantly, the in vitro screening results show that all inhibitors tested show some form of activity against the cultured parasite, although the series II inhibitors are rather more potent than series I, the most potent being **8e** with an ED₅₀ of 30 μM. This is a crucial and very important result that not only reinforces the inhibitor design strategy but also confirms the direction for lead modification. Furthermore, it confirms that the glycolytic pathway is an excellent target for drug design, as even at an early stage of inhibitor identification and modification, a reasonable level of activity is observed against the target parasites.

4. Conclusion

Currently, there is a great need to find new drugs and remedies to combat the growing incidence of parasitic diseases that threaten many African, Asian, Central and Southern American countries.¹ From a weakly binding inhibitor (for *Tb* PFK) as a starting point,⁸ through library design and synthesis, new compounds were identified for both *Tb* PFK and *Lm* PyK. A further round of inhibitor development identified furanose sugar amino amides as a new class of trypanosomal glycolytic pathway inhibitors, with **8e** being the lead against PFK (IC₅₀ = 23 μM) and **8m** the lead against PyK (IC₅₀ = 26 μM). Modelling stud-

Table 3. Results of in vitro inhibitor screenings against *Trypanosoma brucei*

Inhibitor	ED ₅₀ (mM)
2m	0.13
2z	0.83
3b	0.40
3m	1.88
8b	0.11
8e	0.030
8f	0.035

ies on known crystal structures of *Tb* PFK and *Lm* PyK have provided some insight into the possible modes of action of these inhibitors and will help guide lead development and further probing of the respective binding sites. In the case of PyK, effector site probing with specifically designed inhibitors may also provide information as to its allosteric mechanism. Crucially, the effectiveness of the inhibitors against cultured trypanosomatids has not only shown a good level of trypanocidal activity, but confirms the sugar amino amides as prime candidates for lead development.

5. Experimental

5.1. Materials and methods

^1H and ^{13}C NMR were recorded on Bruker AC 250 or AC 360 instruments. Chemical shifts (δ) were recorded in parts per million (ppm) downfield of tetramethylsilane and were referred to residual undeuterated solvent present in the deuterated solvent of the sample (e.g., CH_3OH in CD_3OD). Electrospray ionisation mass spectroscopy (ESI) was carried out on a Micromass VG Platform II instrument. Solvents used were either water or acetonitrile/water (1:1, 0.1% acetic acid) in either positive or negative scan modes. Fast Atom Bombardment (FAB) high resolution mass spectra were recorded on a Kratos MS50TC instrument. Infra-red absorption spectroscopy was performed on a Perkin-Elmer FT-IR Paragon 1000 spectrometer, and ν_{max} values are quoted in cm^{-1} . Optical rotations were performed at room temperature on an AA1000 polarimeter from Optical Activity Ltd (measurements made at the sodium D-line). Concentrations are given in g/100 mL. Thin layer chromatography was performed on Merck DC-Alufolien Kieselgel 60F₂₄₅ 0.2 mm pre-coated plates. Components were visualised by UV fluorescence or by potassium permanganate or ninhydrin stains. Melting points were obtained on Gallenkamp melting point apparatus. Parallel synthesis was performed using the following instruments: Bohdan Neptune reagent dispenser, Bohdan MiniBlock Synthesiser and shaker, and Christ β -RVC solvent evaporator. Mass directed purification was carried out on a Waters ZMD mass spectrometer with Waters 600 HPLC using MassLynx version 3.5 and FractionLynx software. The HPLC column used was a Waters Xterra, C18, 60×21.20 mm, 5 μ microns. Parallel flash column chromatography was carried out using Quad3 parallel purification system using pre-packed columns.

5.1.1. 2,5-Anhydro-D-mannose (1).¹⁰ D-Glucosamine hydrochloride (2.0 g) was dissolved in water (50 mL) and stirred at 0 °C for approximately 5 h. Sodium nitrite (1.6 g, 2.5 equiv) was then added, followed by cautious addition of Amberlite 120 H^+ resin (47 mL), maintaining the temperature between 0 and 5 °C. The reaction was then left to stir at 0 °C for 18 h before the resin was removed by filtration. The solution was then neutralised by portion-by-portion addition of Dowex CO_3^{2-} resin. The resin was re-

moved by filtration and the remaining solution was lyophilised to yield the title compound as a pale yellow hygroscopic solid (1.33 g, 88%). $R_f = 0.42$, $\text{CH}_2\text{Cl}_2/\text{MeOH}$ (8:2) ^1H NMR (D_2O), δ (ppm): 3.50–3.75 (3H, m, H-2, $2 \times$ H-6), 3.78–3.86 (1H, m, H-5), 3.95 (1H, t, $J_{4,3} = J_{4,5} = 5.5$ Hz, H-4), 4.10 (1H, t, $J_{3,4} = J_{3,2} = 5.5$ Hz, H-3), 5.00 (1H, d, $J_{1,2} = 5.5$ Hz, H-1 gem-diol), 8.35 (s, H-1 aldehyde). ^{13}C NMR (D_2O), δ (ppm): 61.2 (C6), 76.8 (C4), 77.8 (C3), 83.2 (C5), 84.6 (C2), 90.0 (C-1 gem-diol).

5.1.2. Synthesis of series I: N-substituted-1-amino-2,5-anhydro-1-deoxy-D-mannitol derivatives (2a–4c).²⁰ Using the Bohdan Neptune reagent manager, a methanolic solution of **1** (0.7 M) was added to 17×2 mL reactors each containing a benzylamine derivative (100 mg, pre-weighed by Sigma–Aldrich Filling Station) in equimolar quantities. The Bohdan MiniBlock synthesiser that contained the reactors was then shaken for 15 min. Sodium cyanoborohydride in methanol (2.4 M, 0.7 equiv) was added to each reactor, before adjusting the pH to 6 by dropwise addition of HCl in methanol (0.5 M). The MiniBlock was then shaken for a further 2 h, monitoring the pH of each reactor, and adjusting the pH if necessary. The reaction mixtures were then transferred to a microtitre plate and the solvent removed under reduced pressure. The residues were dissolved in acetonitrile/water (1:1, 0.1% acetic acid) and purified using mass directed purification.²¹

5.1.3. 2,5-Anhydro-1-deoxy-1-(3,4-dichlorobenzylamino)-D-mannitol (2m). From 3,4-dichlorobenzylamine and using ZMD method 1, yield = 12 mg, 7%. Decomposes >190 °C. ^1H NMR (CD_3OD), δ (ppm): 2.72 (1H, dd, $J_{\text{gem}} = 12.5$ Hz, $J_{1a,2} = 7.5$ Hz, H-1a), 2.79 (1H, dd, $J_{\text{gem}} = 12.5$ Hz, $J_{1b,2} = 3.5$ Hz, H-1b), 3.61–4.03 (8H, m, H-2, H-3, H-4, H-5, $2 \times$ H-6, $2 \times$ ArCH_2), 7.24 (1H, dd, $J_{\text{ArH-ortho}} = 8.0$ Hz, $J_{\text{ArH-meta}} = 2.0$ Hz, ArH), 7.40 (1H, d, $J_{\text{ArH-ortho}} = 8.0$ Hz, ArH), 7.58 (1H, d, $J_{\text{ArH-meta}} = 2.0$ Hz, ArH). ^{13}C NMR (CD_3OD), δ (ppm): 50.1 (C1), 51.3 (Ar-CH_2), 61.5 (C6), 76.9 (C2), 79.2 (C5), 81.7 (C4), 83.5 (C3), 127.4–129.6 (3C, $3 \times$ ArH), 129.9–131.3 (2C, $2 \times$ ArCl), 139.9 (C8, ArC). ESI⁺: $[\text{M}+\text{H}]^+ = 322.1$ [^{35}Cl – ^{35}Cl]. FAB HRMS (+ve) found $m/z = 322.06074$ and 324.05862 $[\text{M}+\text{H}]^+$, $\text{C}_{13}\text{H}_{18}\text{NO}_4\text{Cl}_2$ requires 322.06129 ($2 \times$ ^{35}Cl) and 324.05834 ($^{35}\text{Cl} + ^{37}\text{Cl}$). $[\alpha]_D = +5.7^\circ$ (c 0.7, MeOH).

5.1.4. 2,5-Anhydro-1-deoxy-1-(cycloheptylamino)-D-mannitol (3m). From cycloheptylamine and using ZMD Method 2, yield = 66 mg, 33%. Decomposes >225 °C. ^1H NMR (CD_3OD), δ (ppm): 1.27–1.91 (12H, m, $6 \times$ $-\text{CH}_2\text{-cycloheptane}$), 2.65–2.84 (3H, m, $2 \times$ H-1, CH cycloheptane), 3.60 (1H, dd, $J_{\text{gem}} = 12.0$ Hz, $J_{5,6a} = 5.5$ Hz, H-6a), 3.68 (1H, dd, $J_{\text{gem}} = 12.0$ Hz, $J_{5,6b} = 3.5$ Hz, H-6b), 3.78–3.93 (4H, m, H-2, H-3, H-4, H-5). ^{13}C NMR (CD_3OD), δ (ppm): 23.6 (2C, $2 \times$ cycloheptane), 27.3 (2C, $2 \times$ cycloheptane), 33.0 (2C, $2 \times$ cycloheptane), 48.4 (C1), 58.6 (cycloheptane CH), 61.5 (C6), 77.0 (C4), 79.5 (C3), 81.6 (C2), 84.1 (C5). ESI⁺: $[\text{M}+\text{H}]^+ = 260.2$. FABHRMS (+ve) found $m/z = 260.18594$ $[\text{M}+\text{H}]^+$, $\text{C}_{13}\text{H}_{26}\text{NO}_4$ requires 260.18618. $[\alpha]_D = 6.7^\circ$ (c 1.7, MeOH).

5.1.5. Scale-up method for amines 2m and 3m. The appropriate amine (1.5 equiv) was added to a solution of aldehyde **1** (0.36 g, 1 equiv) in methanol (10 mL) in a solid phase reaction cartridge. The cartridge was sealed and placed on a shaker for 2 h. Borohydride resin (1.17 g, 2 equiv, 3.8 mmol/g) was added and the cartridge was shaken for a further 24 h. 4-Benzyloxybenzaldehyde polystyrene (0.76 g, 1.1 equiv, 3.2 mmol/g) in dichloromethane (4 mL) was added before leaving the reaction to shake for a further 72 h. After ESMS mass spectroscopy (positive) confirmed no more 3,4-dichlorobenzylamine to be present in the solution, the resin was removed by filtration and was washed with methanol (3× 5 mL) and dichloromethane (5 mL). All filtrates were combined and the solvent removed under reduced pressure to yield the title compounds (yield = 84–94%).

5.1.6. *N*-Boc-2,5-anhydro-1-deoxy-1-(3,4-dichlorobenzylamino)-D-mannitol (5a). To a stirred mixture of amine **2m** (0.96 g, 1 equiv) in acetonitrile (10 mL), water was added dropwise until the amine had dissolved. Di-*tert*-butyl dicarbonate (0.64 g, 1 equiv) in dioxane (2 mL) was added and the reaction was cooled to 0 °C. 4-Dimethylaminopyridine (0.091 g, 0.25 equiv) was added then and the reaction was stirred for 2 h. After the addition of water (10 mL), the reaction was extracted in to ethyl acetate (3× 10 mL). The organic layer was washed with sat. NaHCO₃ (2× 10 mL) and the combined aqueous layers were neutralised with 2 M HCl before being re-extracted with ethyl acetate (2× 10 mL). The combined aqueous layers were then acidified to pH 1 before another re-extraction with ethyl acetate (3× 10 mL). All organic layers were combined and washed with 5% NaHSO₄ (2× 5 mL), dried over Na₂SO₄, filtered and the solvent removed under reduced pressure to yield the title compound as a pale yellow oil (0.73 g, 58%). *R*_f = 0.27 CH₂Cl₂/MeOH (9.5:0.5). ¹H NMR (CDCl₃), δ (ppm): 1.34 (9H, s, 9× *t*Bu CH₃), 3.24–3.46 (2H, m, 2× H-1), 3.59–3.73 (2H, m, 2× H-6), 3.75–4.14 (4H, m, H-2, H-3, H-4, H-5), 4.37 (2H, s, 2× ArCH₂), 6.98 (1H, dd, *J*_{ArH-ortho} = 8.0 Hz, *J*_{ArH-meta} = 2.0 Hz, ArH), 7.24 (1H, d, *J*_{ArH-meta} = 2.0 Hz, ArH), 7.32 (1H, d, *J*_{ArH-ortho} = 8.0 Hz, ArH). ¹³C NMR (CDCl₃), δ (ppm): 28.2 (3C, 3× *t*Bu CH₃), 48.2 (C2), 51.0 (ArCH₂), 62.1 (C6), 76.6 (C4), 78.5 (C3), 81.2 (*t*Bu C), 82.3 (C5), 82.9 (C2), 126.4–130.3 (3C, 3× ArH), 131.0–132.3 (2C, 2× ArCl), 132.3 (ArC), 156.6 (Boc carbonyl). ESI⁺: [M+Na]⁺ = 444.2 [³⁵Cl–³⁵Cl]. FTIR thin film (cm^{−1}): 3398 br (OH), 2978 and 2932 (CH), 1672 (C=O).

5.1.7. *N*-Boc-2,5-anhydro-1-deoxy-1-(cycloheptylamino)-D-mannitol (5b). Prepared from **3m** using the same method as for the preparation of **5a** (yield = 0.88 g, 57%). ¹H NMR (CDCl₃), δ (ppm): 1.37–1.78 (21H, m, 6× –CH₂-cycloheptane, 9× *t*Bu CH₃), 3.05–3.39 (2H, m, 2× H-1), 3.64–4.32 (7H, m, H-2, H-3, H-4, H-5, 2× H-6, CH cycloheptane). ¹³C NMR (CDCl₃), δ (ppm): 23.5–27.8 (4C, 4× cycloheptane), 28.3 (3C, 3× *t*Bu CH₃), 33.2–35.3 (2C, 2× cycloheptane), 47.2 (C1), 60.9 (cycloheptane CH), 62.6 (C6), 77.0 (C4), 78.4 (C3), 80.4 (*t*Bu C), 83.4 (C5), 83.6 (C2), 156.9 (Boc carbonyl). ESI⁺: [M+Na]⁺ = 382.1.

5.1.8. *N*-Boc-2,5-anhydro-1-deoxy-1-(3,4-dichlorobenzylamino)-D-mannonic acid (6a). *N*-Boc protected amine **5a** (0.13 g, 1 equiv) and TEMPO (3 mg, 6 mol%) were dissolved in CH₂Cl₂ (1 mL). A solution of KBr (0.4 M), tetrabutylammonium chloride (0.3 M) in sat. NaHCO₃ (1 mL) was added and the solution was cooled to 0 °C and stirred vigorously. A solution of sodium hypochlorite (1.3 M, 0.75 mL), sat. NaHCO₃ (0.33 mL) and brine (0.66 mL) were added dropwise over a period of 30 min. The reaction was then allowed to stir for a further 2 h. The two layers were then separated and the organic phase was washed with water (3× 10 mL). The aqueous layers were combined and acidified to pH 1 with HCl (2 M) before extracting with ethyl acetate (3× 10 mL). The organic layer was then dried over Na₂SO₄, filtered and the solvent removed under reduced pressure to yield the title compound as an off white solid (97 mg, 72%). Decomposes >150 °C. FTIR thin film (cm^{−1}): 3417 br (OH), 2978 and 2932 (CH), 1667 (2× C=O). ¹H NMR (CDCl₃), δ (ppm): 1.47 (9H, s, 9× *t*Bu CH₃), 3.24–3.47 (2H, m, 2× H-1), 3.84–4.40 (6H, m, H-2, H-3, H-4, H-5, 2× ArCH₂), 5.93 (1H, s broad, acid OH), 6.98 (1H, d, *J*_{ArH-ortho} = 7.5 Hz, ArH), 7.24 (1H, s, ArH), 7.31 (1H, d, *J*_{ArH-ortho} = 7.5 Hz, ArH). ¹³C NMR (CDCl₃), δ (ppm): 28.2 (3× *t*Bu CH₃), 48.0 (C1), 51.0 (ArCH₂), 78.0 (C4), 79.7 (C3), 81.5 (*t*Bu C), 81.8 (C5), 83.9 (C2), 126.5–130.3 (3C, 3× ArH), 131.0–132.3 (2C, 2× ArCl), 138.3 (ArC), 156.4 (Boc carbonyl), 174.1 (acid). ESI[−]: [M–H][−] = 434.1 [³⁵Cl–³⁵Cl].

5.1.9. *N*-Boc-2,5-anhydro-1-deoxy-1-(cycloheptylamino)-D-mannonic acid (6b). Prepared from **5b** using the same method as for the preparation of **6a** with the stir time increased from 2 to 24 h (yield = 0.19 g, 38%). ¹H NMR (CDCl₃), δ (ppm): 1.38–1.74 (21H, m, 6× –CH₂-cycloheptane, 9× *t*Bu CH₃), 3.18–3.41 (2H, m, 2× H-1), 3.42–5.06 (5H, m, H-2, H-3, H-4, H-5, cycloheptane CH). ESI[−]: [M–H][−] = 372.1.

5.1.10. Synthesis series II: *N,N'*-substituted-1-amino-2,5-anhydro-1-deoxy-1-D-mannonamide derivatives. Part 1: amine coupling (7a–7n).²² The *N*-Boc protected sugar amino acids **6a** and **6b** (1 equiv) were dissolved in CH₂Cl₂ (1 mL) and placed into 10 mL reaction tubes (6× **90**, 7× **91**). To each tube a different amine was added (1 equiv, 7 amines used in total) along with EDCI (1.3 equiv), HOBt (1.5 equiv) and DIPEA (2.2 equiv). The reactions were allowed to stir for 20 h before quenching with NaCl (2 M, 1 mL). For each reaction, the two phases were separated and the aqueous phase extracted with CH₂CH₂ (2× 2 mL). The organic phases were combined and washed with water (2× 2 mL) and HCl (0.5 M, 2× 2 mL). The solutions were then dried over Na₂SO₄, filtered and the solvent removed under reduced pressure to yield the crude products. The compounds were purified using the Quad3 parallel purification system, using pre-packed columns, eluting with CH₂Cl₂/MeOH (9.5:0.5). Solvent removal yielded the desired compounds.

5.1.11. *N*-Boc-2,5-Anhydro-1-deoxy-1-(3,4-dichlorobenzylamino)-D-3,4-dichlorobenzylmannonamide (7e). From 3,4-dichlorobenzylamine and **6a**, yield = 33 mg, 25%. *R*_f = 0.14 CH₂Cl₂/MeOH (9.5:0.5). ¹H NMR (CDCl₃),

δ (ppm): 1.39 (9H, s, $9 \times t\text{Bu CH}_3$), 3.28–3.48 (2H, m, $2 \times \text{H-1}$), 3.81–4.41 (8H, m, H-2, H-3, H-4, H-5, $4 \times \text{ArCH}_2$), 6.99 (2H, $2 \times \text{ArH}$), 7.20–7.32 (4H, m, $4 \times \text{ArH}$).

5.1.12. Synthesis of series II: Synthesis of *N,N'*-substituted-1-amino-2,5-anhydro-1-deoxy-1-D-mannonamide derivatives. Part 2: Boc-deprotection (8a–8n).²³ Boc-protected amino mannonamides (from part 1) were dissolved in CH_2Cl_2 (1.5 mL). Trifluoroacetic acid (1 mL) was added and the reactions were stirred for 2 h. The solvent was then removed under reduced pressure and the residue dissolved in acetonitrile/water (1:1, 0.1% acetic acid) and purified using mass directed purification (ZMD Method 1). The removal of the solvent by lyophilisation afforded the desired compounds.

5.1.13. 2,5-Anhydro-1-deoxy-1-(3,4-dichlorobenzylamino)-D-3,4-dichlorobenzylmannonamide (8e). From **7e**, yield = 16 mg, 58%. ^1H NMR (CD_3OD), δ (ppm): 3.28 (1H, dd, $J_{\text{gem}} = 13.0$ Hz, $J_{1a,2} = 3.0$ Hz, H-1a), 3.46 (1H, dd, $J_{\text{gem}} = 13.0$ Hz, $J_{1b,2} = 9.5$ Hz, H-1b), 4.01 (1H, t, $J_{2,3} = J_{3,4} = 1.51$ Hz, H-3), 4.24–4.34 (4H, m, $4 \times \text{ArCH}_2$), 4.38 (1H, s, NH amine), 4.42 (1H, t, $J_{3,4} = J_{4,5} = 1.5$ Hz, H-4), 4.44–4.48 (1H, m, H-2), 4.51 (1H, d, $J_{4,5} = 1.5$ Hz, H-5), 7.19–7.27 (2H, m, $2 \times \text{ArH}$), 7.41–7.73 (4H, m, $4 \times \text{ArH}$), 8.54 (1H, t, $J_{14, \text{NH-amide}} = 6.5$ Hz, NH-amide). ESI^+ : $[\text{M}+\text{H}]^+ = 493.1$ [$^{35}\text{Cl}-^{35}\text{Cl}-^{35}\text{Cl}-^{35}\text{Cl}$].

5.1.14. Activity screens against Tb PFK. In a 1 mL cuvette was placed an inhibitor solution (40 μL , made up with 0.1 M triethanolamine buffer, pH 8.0), 12.5 μg /mL PFK (16 μL), made up to 760 μL with 0.1 M triethanolamine, pH 8.0 and was incubated for 2 min. The reaction was started by the addition of the substrate mix (40 μL , 40 mM MgCl_2 , 40 mM F6P, 20 mM ATP, 6 mM NADH, 18 U/mL aldolase [Sigma], 20 U/mL triosephosphate isomerase [Sigma] and 34 U/mL glycerol-3-phosphate dehydrogenase [Sigma]), gently agitated and the decrease in absorbance at 340 nm measured for 2 min (using Lambda Bio). The initial rate was then calculated using UV kinlab. A control rate with no inhibitor present was also determined. The rate for each inhibitor assay was expressed as a percentage of the control assay. All compounds considered as hits were screened against the coupling enzymes alone to avoid a false positive result. All compounds were found to inhibit PFK only.

5.1.15. Activity screens against Lm PyK. To a 1 mL cuvette was added the substrate mix (500 μL , 50 mM triethanolamine buffer, pH 7.2, 50 mM KCl, 6 mM MgSO_4 , 0.6 mM ADP, 0.84 mM NADH, 27.6 units/mL lactate dehydrogenase [Roche]), 0.04 mg/mL PyK (10 μL), an inhibitor solution (50 μL , made up with 0.1 M triethanolamine, pH 7.5) and made to 992 μL by the addition of water. The mixture was incubated for 2 min before the reaction was started by the addition of 50 μM PEP (50 μL). The mixture was gently agitated and the decrease in absorbance at 340 nm was measured for 2 min (using Lambda Bio). The data were processed in the same manner as for the screen against PFK. All compounds considered as hits were screened against

the coupling enzymes alone to avoid a false positive result. All compounds were found to inhibit PyK only.

5.1.16. In vivo screens against *Trypanosoma brucei*. The anti-trypanosomal activity tests were performed according to the procedure previously reported by Hoet et al.²⁴ using cultured bloodstream-form cells of strain *T. brucei* 427. A 76-h incubation time was selected.

Acknowledgments

We thank various labworkers and honours students who helped during the course of this project, particularly José Martinez-Oyanedel and Marcos Navarro. This work was supported by the European Commission under its INCO-DEV programme.

Supplementary data

Supplementary data associated with this article can be found, in the online version, at [doi:10.1016/j.bmc.2008.03.045](https://doi.org/10.1016/j.bmc.2008.03.045).

References and notes

- Verlinde, C. L. M. J.; Hannaert, V.; Blonski, C.; Willson, M.; Périé, J. J.; Fothergill-Gilmore, L. A.; Oppendoes, F. R.; Gelb, M. H.; Hol, W. G. J.; Michels, P. A. M. *Drug Res. Updates* **2001**, *4*, 50.
- Albert, M. A.; Haanstra, J. R.; Hannaert, V.; Van Roy, J.; Oppendoes, F. R.; Bakker, B. M.; Michels, P. A. *J. Biol. Chem.* **2005**, *280*, 28306.
- Fernandes, A. P.; Nelson, K.; Beverley, S. M. *Proc. Natl. Acad. Sci. U.S.A.* **1993**, *90*, 11608.
- Fothergill-Gilmore, L. A.; Michels, P. A. M. *Prog. Biophys. Mol. Biol.* **1993**, *59*, 105.
- Michels, P. A. M.; Chevalier, N.; Oppendoes, F. R.; Rider, M. H.; Rigden, D. J. *Eur. J. Biochem.* **1997**, *250*, 698.
- Van Schaftingen, E.; Oppendoes, F. R.; Hers, H. G. *Eur. J. Biochem.* **1985**, *153*, 403.
- Martinez-Oyanedel, J.; McNae, I. W.; Nowicki, M. W.; Keillor, J. W.; Michels, P. A. M.; Fothergill-Gilmore, L. A.; Walkinshaw, M. D. *J. Mol. Biol.* **2007**, *366*, 1185.
- Claustre, S.; Denier, C.; Lakhdar-Ghazal, F.; Lougare, A.; Lopez, C.; Chevalier, N.; Michels, P. A. M.; Périé, J.; Willson, M. *Biochemistry* **2002**, *41*, 10183.
- Rigden, D. J.; Phillips, S. E. V.; Michels, P. A. M.; Fothergill-Gilmore, L. A. *J. Mol. Biol.* **1999**, *291*, 615.
- Claustre, S.; Bringaud, F.; Azéma, L.; Baron, R.; Périé, J.; Willson, M. *Carbohydr. Res.* **1999**, *315*, 339.
- Horton, D.; Philips, K. D. *Carbohydr. Res.* **1973**, *30*, 367.
- Piper, I. M.; MacLean, D. B.; Kvarnstrom, I.; Szarek, W. A. *Can. J. Chem.* **1983**, *61*, 2721.
- Booth, R. J.; Hodges, J. C. *J. Am. Chem. Soc.* **1997**, *119*, 4882.
- Booth, R. J.; Hodges, J. C. *Acc. Chem. Res.* **1999**, *32*, 18.
- Kaldor, S. W.; Siegel, M. G.; Fritz, J. E.; Dressman, B. A.; Hahn, P. J. *Tetrahedron Lett.* **1996**, *37*, 7193.
- Davis, N. J.; Flitsch, S. L. *Tetrahedron Lett.* **1993**, *34*, 1181.
- Furka, A.; Sebestyen, F.; Asgedom, M.; Dibo, G. *Int. J. Pept. Prot. Res.* **1991**, *37*, 487.
- Han, S.-Y.; Kim, Y.-A. *Tetrahedron* **2004**, *60*, 2447.
- Shirakihara, Y.; Evans, P. R. *J. Mol. Biol.* **1988**, *204*, 973.

19. Fothergill-Gillmore, L. A.; Rigden, D. J.; Michels, P. A.; Phillips, S. E. *Biochem. Soc. Trans.* **2000**, 28, 86.
20. Characterisation data for this series can be found in the [supplementary data](#). Only characterisation for the main compounds **2m** and **3m** are given here.
21. Details of mass directed purification methods can be found in the [supplementary material](#).
22. Characterisation data for this series can be found in the [supplementary data](#). Only characterisation for the compound **7e** is given here. Due to low yields and amounts of material, characterisation for this part was minimal.
23. Characterisation data for this series can be found in the [supplementary data](#). Only characterisation for the compound **8e** is given here.
24. Hoet, S.; Stévigny, C.; Block, S.; Opperdoes, F.; Colson, P.; Baldeyrou, B.; Lansiaux, A.; Bailly, C.; Quentin-Leclercq, J. *Planta Med.* **2004**, 70, 407.